Supplementary Materials

Tunable multi-doped carbon nanofiber air cathodes based on Poly(ionic liquid) for sodium oxygen batteries with diglyme/ionic liquid-based hybrid electrolytes

Han Li [a+], The An Ha [b+], Nagore Ortiz-Vitoriano [c, d], Xungai Wang [a], Jian Fang [e*], Patrick C. Howlett [b], Cristina Pozo-Gonzalo [b**]

+Author equal contribution

[a]*Institute for Frontier Materials, Deakin University, Geelong, Victoria, 3200, Australia*

[b]*ARC Centre of Excellence for Electromaterials Science, Institute for Frontier Materials, Deakin University, Burwood, Victoria, 3125, Australia*

[c]*Centre for Cooperative Research on Alternative Energies (CIC energiGUNE), Basque Research and Technology Alliance (BRTA), Parque Tecnológico de Alava, Albert Einstein 48, 01510 Vitoria-Gasteiz, Spain*

[d]*Ikerbasque, Basque Foundation for Science, María Díaz de Haro 3, 48013 Bilbao, Spain*

[e]*College of Textile and Clothing Engineering, Soochow University, Suzhou, JiangSu, 215123, P. R. China*

[*]Corresponding author. E-mail address: jian.fang@suda.edu.cn (J. Fang).

[**]Corresponding author. E-mail address: cpg@deakin.edu.au (C. Pozo-Gonzalo).

1 Experimental section

1.1 Chemicals

Poly(diallyldimethylammonium) bis(fluorosulfony)imde (PDADMAFSI, Mw=400 000-500 000 g mol^{-1}) (99.9%, purity) (impurities: 1000 ppm of chloride, 30 ppm of potassium) was prepared by the method previously reported.[1] N, N-dimethyl formamide (DMF) and polyacrylonitrile (PAN, Mw=150 000 g mol^{-1}) were obtained from Sigma-Aldrich Australia. All chemicals were used as received. N-butyl-N-methylpyrrolidinium bis(trifluoromethylsulfonyl)imide ([C_4mpyr][TFSI], 99.9%) and sodium bis(trifluoromethylsulfonyl)imide (NaTFSI, 99.9%) were purchased from Solvionic SA. Diethylene Glycol dimethyl ether (G2, 99.5%) was purchased from Sigma-Aldrich and dried over molecular sieves (3Å) for two weeks in an Argon glovebox (Korea Kiyon, with nominal levels of oxygen and water below 1 ppm) before use. These chemicals were all stored in the Argon filled glovebox, and directly used as received.

Three different compositions of electrolyte were prepared: a 16.6 mol % (ca. 0.4 mol kg^{-1}) NaTFSI in [C_4mpyr][TFSI] (IL) electrolyte solution was prepared by adding NaTFSI (88.5 mg, ca. 0.29 mmol) into [C_4mpyr][TFSI] (621.0 mg, ca. 1.47 mmol) in the Argon filled glovebox for 24 h; a 16.6 mol % NaTFSI in G2 electrolyte was obtained by adding NaTFSI (264.1 mg, ca. 0.87 mmol) into G2 (586.4 mg, ca. 4.4 mmol) and magnetically stirring for 24 h in the Argon filled glovebox; a 16.6 mol % NaTFSI in G2/[C_4mpyr][TFSI] hybrid electrolyte was prepared by adding NaTFSI (205.0 mg, ca. 0.68 mmol) into [C_4mpyr][TFSI] (287.0 mg, ca. 0.68 mmol) and G2 (364.7 mg, ca. 2.7 mmol) magnetically stirring for 24 h in the Argon filled glovebox. Later, all the electrolytes were dried on a Schlenk line at 50 °C for 1 h and further at 70 °C for 24 h. The water content of as-prepared electrolyte was <20 ppm as per Karl Fischer titration measurement (Metrohm KF 831 Karl Fischer coulometer).

1.2 PAN:PDADMA FSI-based carbon nanofibers synthesis

The PAN:PDADMA FSI carbon nanofibers were prepared by electrospinning along with pre-oxidation and pyrolysis process, following the same procedures previously reported.[2] As representative, 0.27 g PDADMA FSI and 0.63 g PAN were added in DMF (10 mL) and the

obtained solution was magnetically stirred at 50℃ to form a homogenous viscous solution. The electrospinning process of PAN/PDADMA FSI/DMF solution was carried out at 0.6 mL h^{-1} of flow rate for 5 h using flat tip needle (21G) as the spinning head and a DC power supply (Gamma, FL 32174) was used to apply high voltage of 15 kV. A metal roller (10 cm in length and 5.5 cm in diameter) with rotation rate of 350 rpm used as ground drum collector was placed at a distance of 15 cm from the tip of needle. The as-spun nanofibers were then pre-oxidized at 250 ℃ with a ramp rate of 2.5 ℃ min^{-1} for 1.5 h under air flow, and then pyrolyzed at 800 ℃ with a heating rate of 5 ℃ min^{-1} for 1 h under nitrogen atmosphere in a tube furnace (Labec, HTFS60-300/12). Finally, the PAN:PDADMA FSI-based carbon nanofibers were obtained. All the experimental processes were conducted at the same procedures with a relative humidity of 40% and at room temperature (25 ℃).

Moreover, to adjust the porosity and heteroatom doping level of the samples, controlled experiments about the fabrication of various PAN:PDADMA FSI-based carbon nanofibers were performed through changing the PAN:PDADMA FSI ratio in the precursor solution (0.9 g PAN; 0.72 g PAN + 0.18 g PDADMA FSI; 0.63 g PAN + 0.27 g PDADMA FSI; 0.54 g PAN + 0.36 g PDADMA FSI). The synthesized products were denoted as PAN:PDADMA FSI 100:0, PAN:PDADMA FSI 80:20, PAN:PDADMA FSI 70:30, PAN:PDADMA FSI 60:40, respectively. Particularly, the preparation of PAN:PDADMA FSI 100:0 (pristine CNFs) was conducted as the control samples to intuitively analyze the effect of PDADMA FSI within the carbon nanofibers. Without specific notifications, all the samples were prepared under the same conditions using the same volume of the precursor solution (3ml), and then carbonized at 800 ℃ for 1h.

The PAN:PDADMA FSI 70:30 with different thickness were prepared through pyrolysis of the as-spun nanofibers with different precursor volumes (3ml, 5ml and 10 ml) for the electrospinning process. The obtained products were carbonized at 800 ℃ for 1h which led to air cathodes with different thickness (e.g., 108 μm, 230 μm and 310 μm).

2 Characterizations of material and discharge products

The surface morphologies of as-spun and carbonized materials were obtained by a Zeiss SUPRA 55VP scanning electron microscope (SEM) at 5 kV working voltage. The microstructures of the carbonized materials were studied by using Transmission electron microscopy (TEM; JEOL 2100F Field Emission transmission electron microscope), while element analysis was performed using the equipped energy-dispersive X-ray spectroscopy (EDS) detector with the spot resolution of 0.24 nm and the energy resolution of 138 eV. The amorphous and graphitic structures of the carbonized materials were examined by Raman spectroscopy with an incident laser light (514 nm wavelength). The nitrogen adsorption-desorption isotherms (Quantachrome Instruments Autosorb-iQ3) were conducted to characterize the porous structures of the materials and Brunauer-Emmett-Teller (BET) method was employed to characterize the specific surface area. A KRATOS Axis Ultra HAS instrument with Al Kα radiation was performed to collected X-ray photoelectron spectroscopy (XPS) data. The energy calibration was referenced to the low binding energy component of the C1s peak at 284.6 eV and Casa XPS software was used to analyze all XPS data.

The morphologies and compositions of the discharge products were characterized by SEM (JOEL JSM IT300 Oxford) equipped with EDS (Energy Dispersive X-ray Spectroscopy). The Na-O_2 battery was first discharge in a bespoke O_2/N_2 glovebox (below 100 ppm of water) and sealed in a canister, and then transferred to an Argon glovebox to characterize the discharge products. In the Argon glovebox, the battery was disassembled and dry THF was used to wash the cathode, in accordance with the previously reported procedure.[3] After dried for 5 min at room temperature, the cathode was placed in an air-tight holder and then transferred into a SEM vacuum chamber. For Raman measurements, after washing with THF, the dried sample was stored in an air-tight sample holder equipped with a microscope slide, a cover slide and a cover slip for laser transmission. Raman spectroscopy of the discharge products within the fibre electrodes was conducted with a Renishaw InVia Raman spectrometer (632 nm).

3 Electrochemical performance

After punched into discs, the air cathodes (diameter of 7 mm) were cleaned with ethanol and dried in a vacuum oven at 120 °C for 24 h. An house-made three-electrode half-cell with continuous oxygen flow was used, as reported previously by Zhang et al.[4] (Fig. S2†). In this

cell, a platinum wire coil was used as the counter electrode and the cathode was working electrode, while a reference electrode was a silver wire immersed in a 5 mM silver trifluoromethanesulfonate in [C_4mpyr][TFSI] solution. The reference electrode was calibrated versus ferrocene ($E_{1/2}$ = + 0.40 V). The volume of the electrolyte in this configuration was 500 μL. The potentials in the discharge and charge plots were reported vs Na^0/Na^+ potential (-2.98 V vs Fc^0/Fc^+). The three-electrode electrochemical measurements were conducted in a bespoke O_2/N_2 glovebox (20.5% oxygen in nitrogen, below 100 ppm water), by using a Biological VMP3/Z multi-channel potentiostat at a current density of 0.6 mA cm^{-2}.

A modified Swagelok cell was used for all the full cell electrochemical experiments, which was prepared in an argon glovebox. Firstly, part of electrolyte (70 μL) was added to four Solupor separators (PI30811B-A1-00-D02, 140 μm in thickness, Lydall Performance Materials), and then another part of electrolyte (30 μL) was added to the air cathodes. In order to remove surface impurities, sodium metal foil (Sigma Aldrich, 99.9%) with a diameter of 10 mm was washed with cyclohexane. The separators with a diameter of 12.7 mm were placed between the air cathodes (diameter of 12.7 mm) and the sodium metal discs (diameter of 10 mm). Before experiments, pure oxygen (ultrahigh purity oxygen grade >99.999% oxygen, <5 ppm moisture, and <3 ppm hydrocarbon gas, Supagas Australia) was used to flush the assembled cells and then all cells rested for 3 h at room temperature. A Biologic VMP 300 multichannel potentiostat, operated at 1.6-3.6 V vs Na^0/Na^+ at 0.1 mA cm^{-2}, was used for the galvanostatic tests.

4 DFT calculations

DFT calculations, containing structural optimization and electronic performances, were conducted under the Materials Studio 8.0, Dmol3 modulus. The electron-electron interaction was depicted by Projector augmented wave (PAW) method with the generalized gradient approximation (GGA) based on the Perdew-Burke-Ernzerhof (PBE) exchange-correlation functional.[5] The energy cutoff was set as 380 eV and the Brillouin zone was sampled with a K-point grid of 4 × 4 × 4. SCF tolerance was 2.0*10-5 eV/atom, and maximum force was 0.05 eV/ Å, while maximum stress was 0.1 GPa. Moreover, maximum displacement was set as 0.005 Å. All atoms were relaxed, and then the intermediates of NaO_2 groups have been absorbed on

the substrates' surface. The electrochemical model of 4 steps of chemical reactions were described as following:[6]

$$4(Na^+ + e^-) + 4\ O_2 \rightarrow 3(Na^+ + e^-) + 3\ O_2 + NaO_2^* \quad (1)$$

$$3(Na^+ + e^-) + 3\ O_2 + NaO_2^* \rightarrow 2(Na^+ + e^-) + 2\ O_2 + 2NaO_2^* \quad (2)$$

$$2(Na^+ + e^-) + 2\ O_2 + 2NaO_2^* \rightarrow (Na^+ + e^-) + O_2 + 3NaO_2^* \quad (3)$$

$$(Na^+ + e^-) + O_2 + 3NaO_2^* \rightarrow 4NaO_2^* \quad (4)$$

Gibbs free energy change (ΔG) of each chemical reaction is calculated by:[7]

$$\Delta G = \Delta E + \Delta ZPE - T\Delta S \quad (5)$$

where E denotes the calculated total energy, ZPE reveals zero point energy, T indicates temperature and S exhibits entropy, respectively. Here, T = 25 ^oC is considered.

5 Supporting Figures

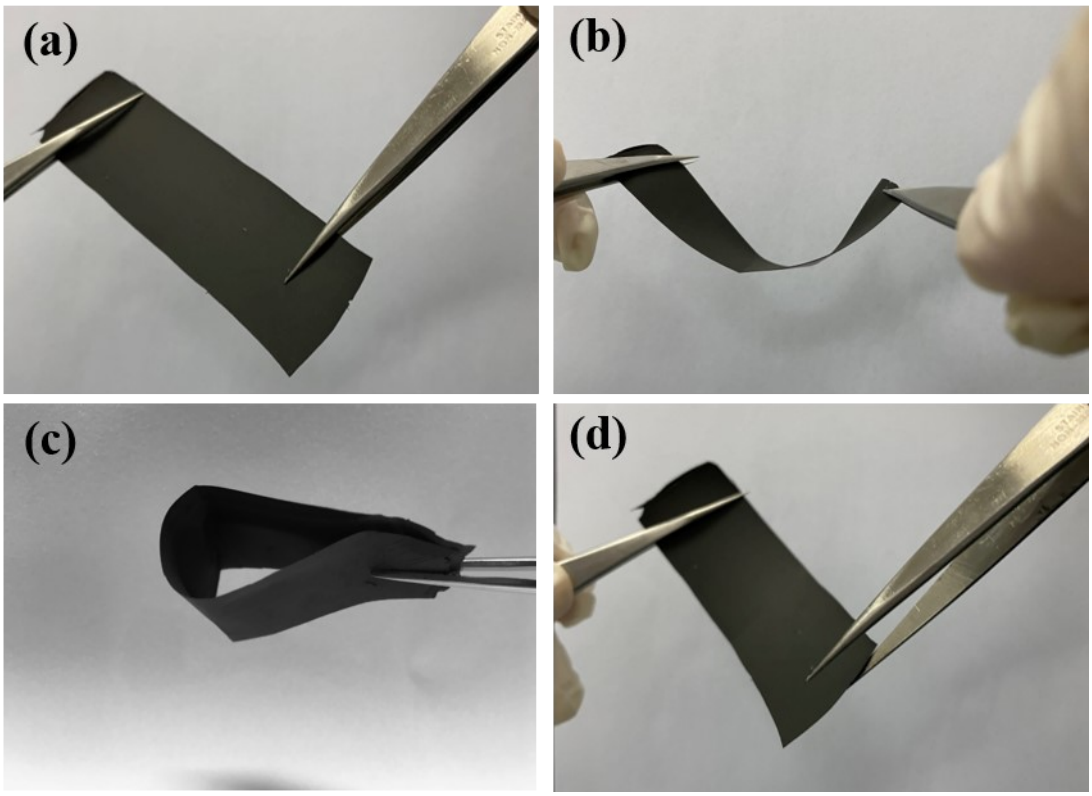

Fig. S1. Photographs of PAN:PDADMA FSI 70:30 with 108 μm in thickness being bent and folded.

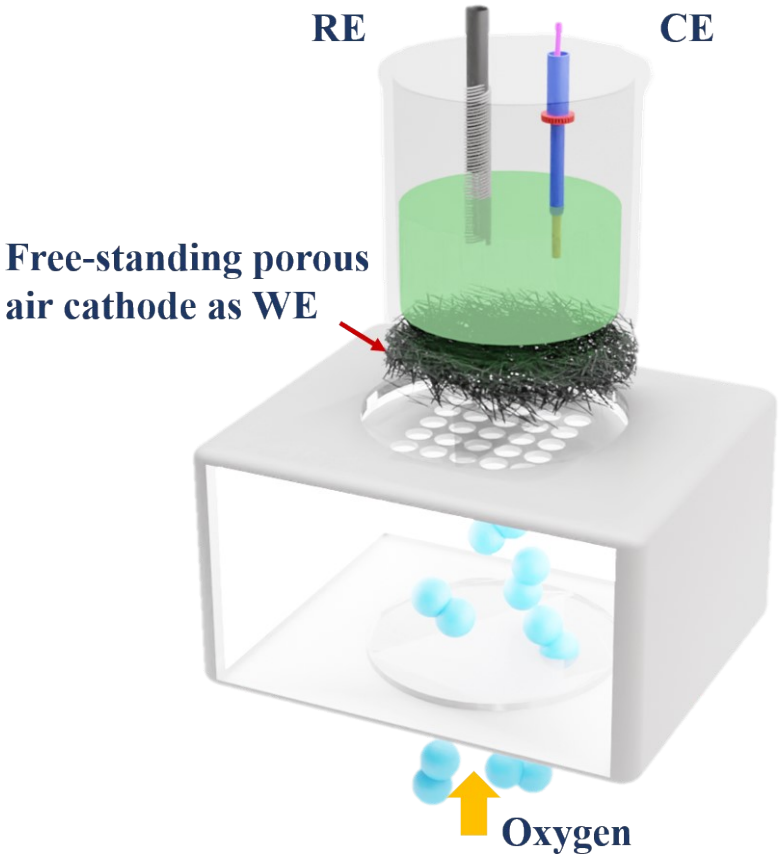

Fig. S2. Schematic illustration of a home-made three-electrode Na-O_2 half-cell.

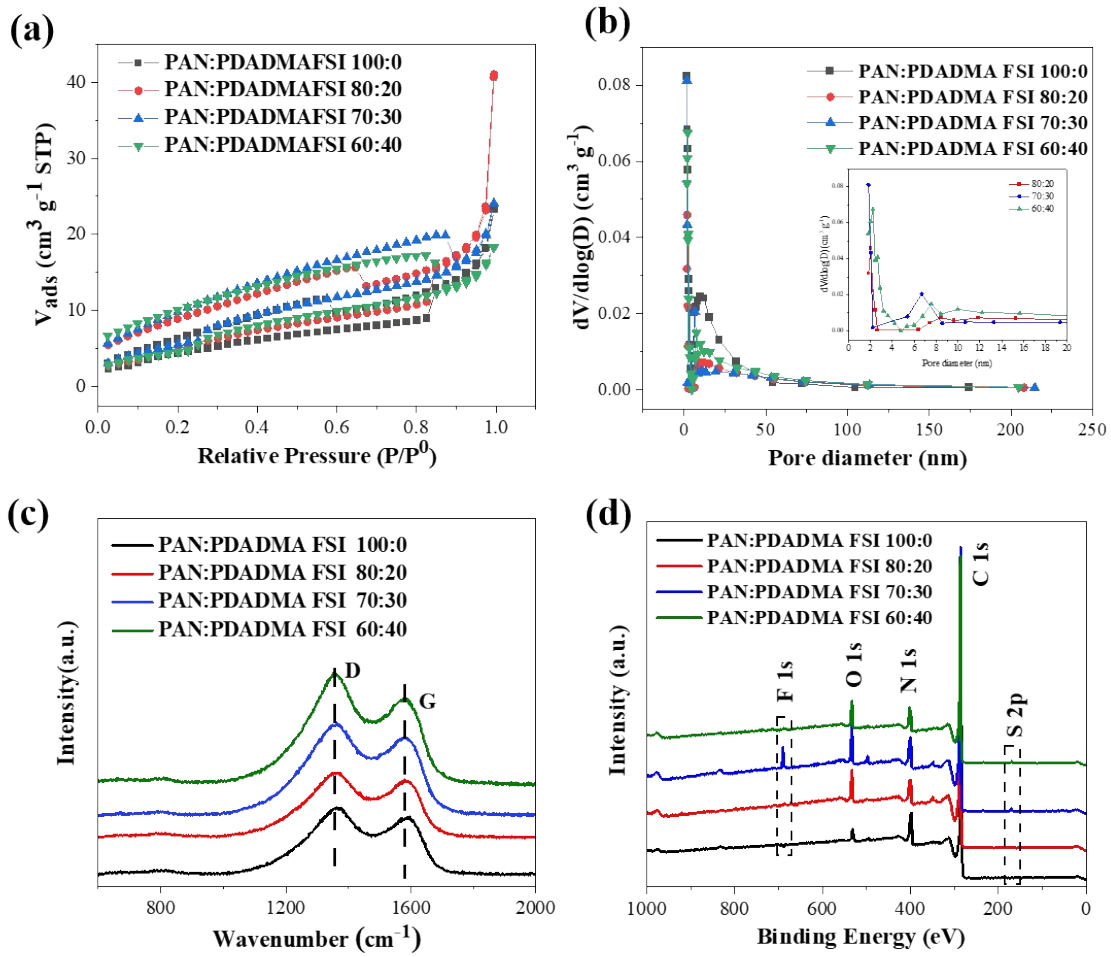

Fig. S3. a) Nitrogen sorption isotherms and b) corresponding pore size distribution, c) Raman spectrum and d) XPS survey spectra of PAN:PDADMA FSI with different ratio weight.

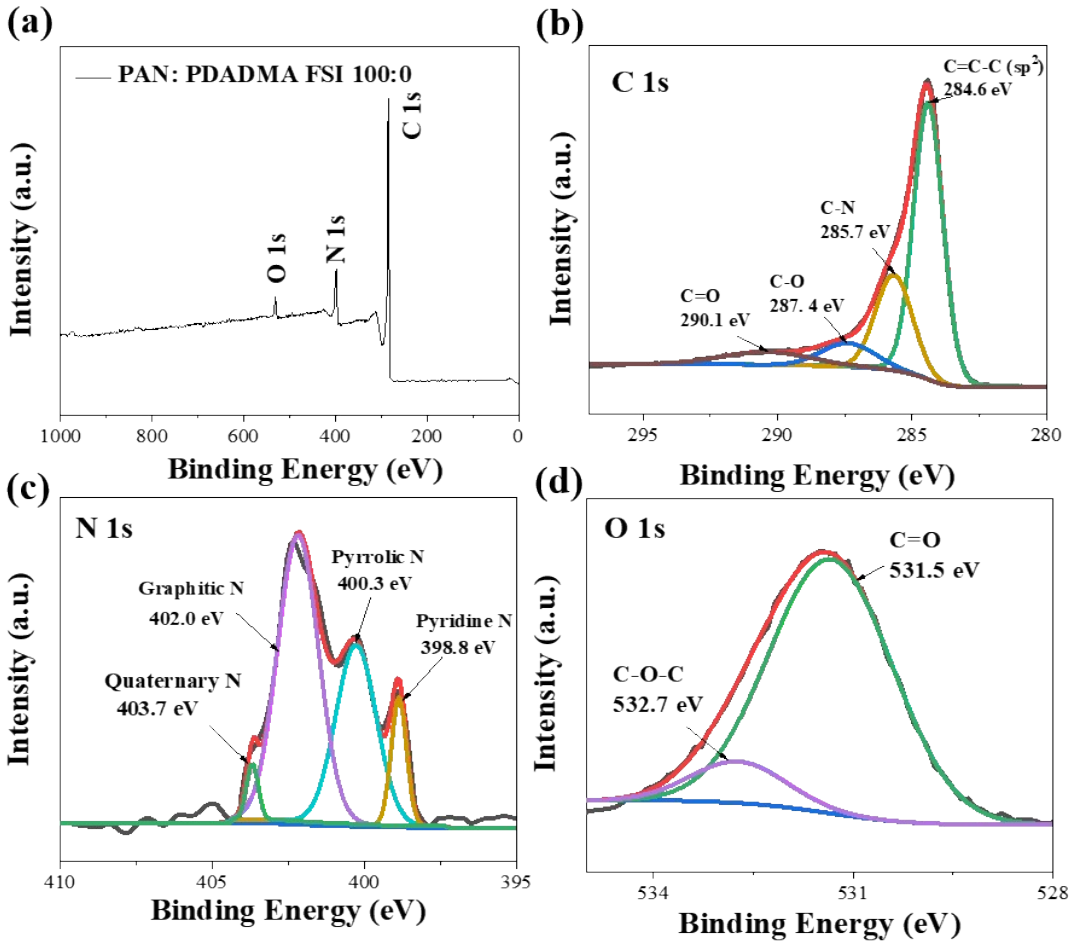

Fig. S4. a) XPS survey spectra and High-resolution XPS spectra of b) C 1s, c) N 1s and d) O 1s of PAN:PDADMA FSI 100:0.

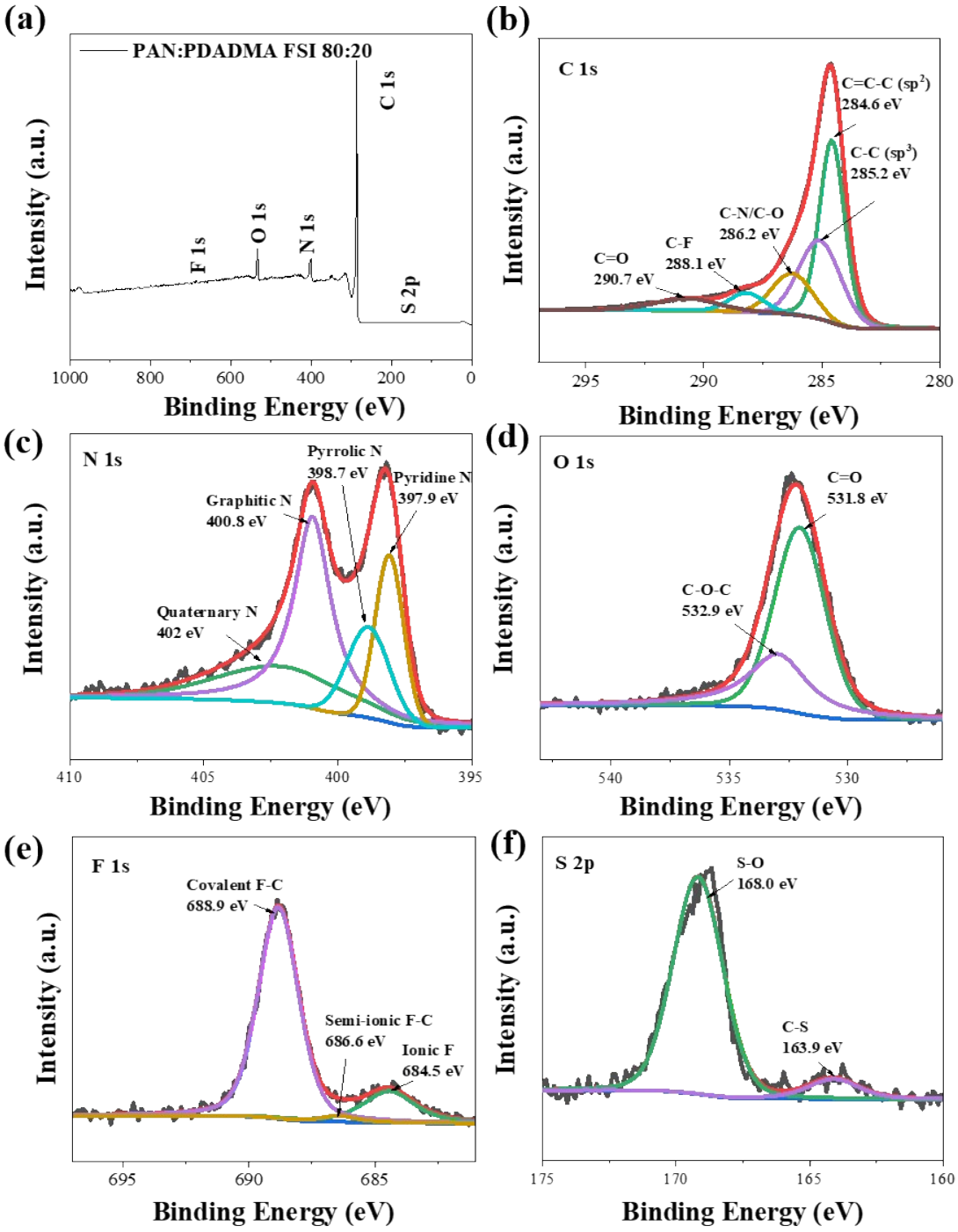

Fig. S5. a) XPS survey spectra and High-resolution XPS spectra of b) C 1s, c) N 1s, d) O 1s, e) F 1s and f) S 2p of PAN:PDADMA FSI 80:20.

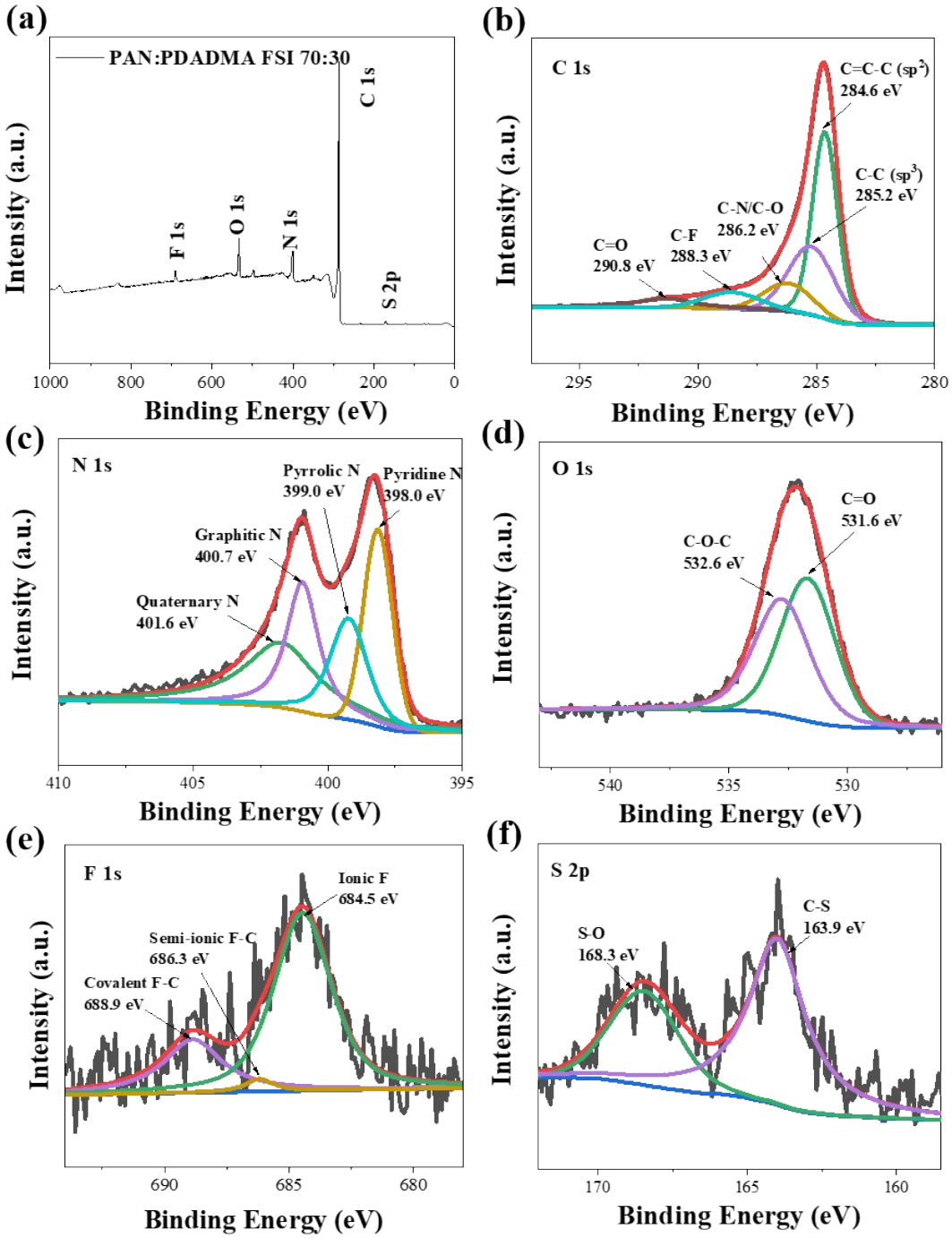

Fig. S6. a) XPS survey spectra and high-resolution XPS spectra of b) C 1s, c) N 1s, d) O 1s, e) F 1s and f) S 2p of PAN:PDADMA FSI 70:30.

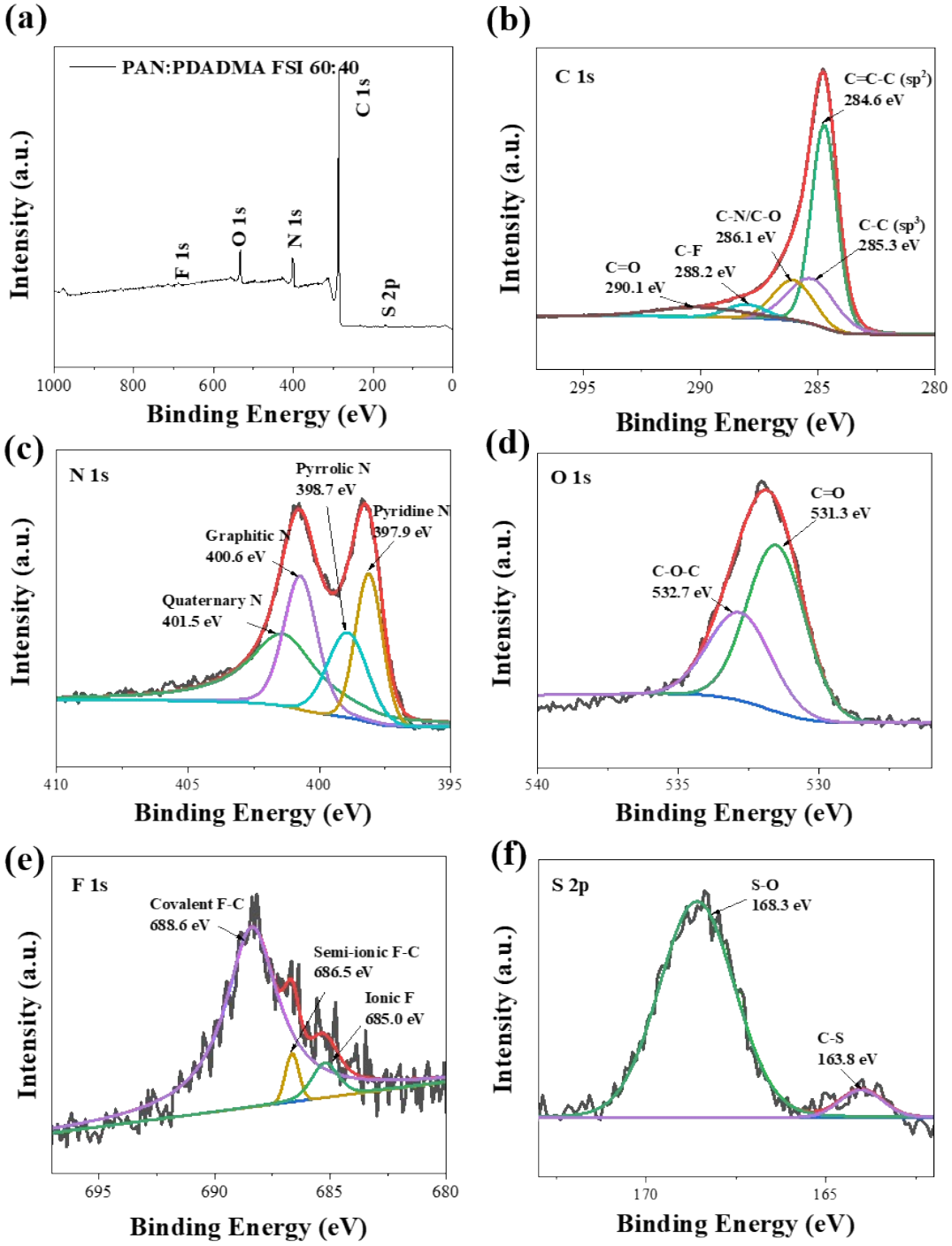

Fig. S7. a) XPS survey spectra and high-resolution XPS spectra of b) C 1s, c) N 1s, d) O 1s, e) F 1s and f) S 2p of PAN:PDADMA FSI 60:40.

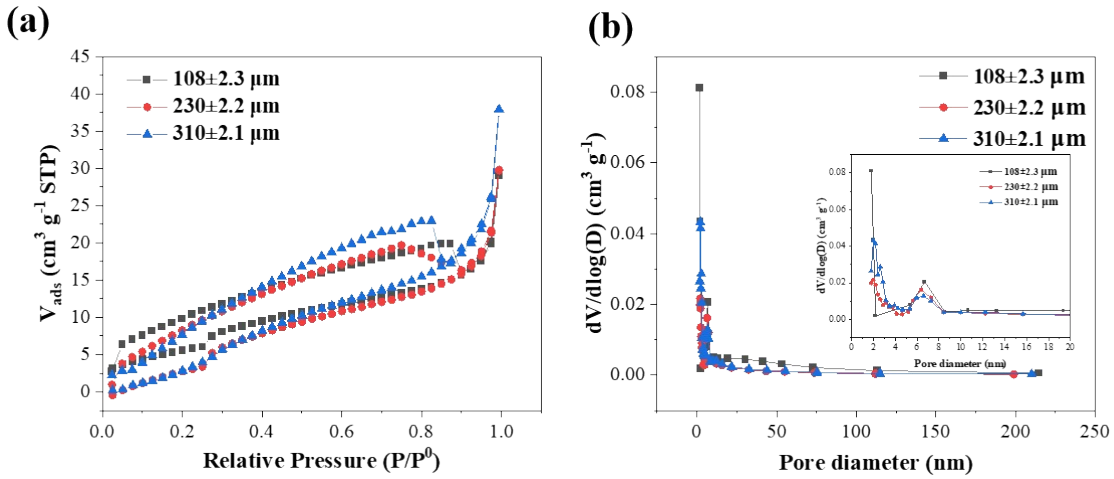

Fig. S8. a) Nitrogen sorption isotherms and b) pore size distribution of PAN: PDADMA FSI 70:30 with different thickness.

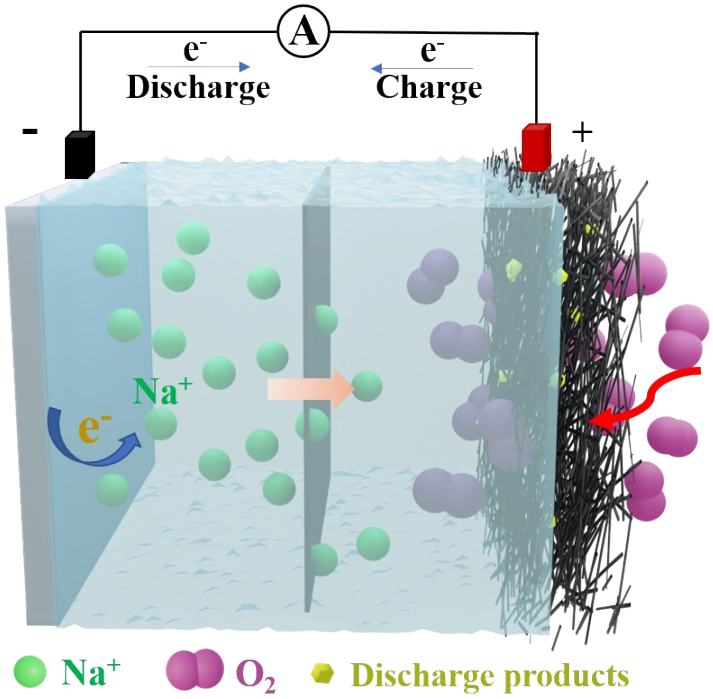

Fig. S9. Schematic illustration of a Na-O_2 battery with PAN:PDADMA FSI as free-standing air cathode.

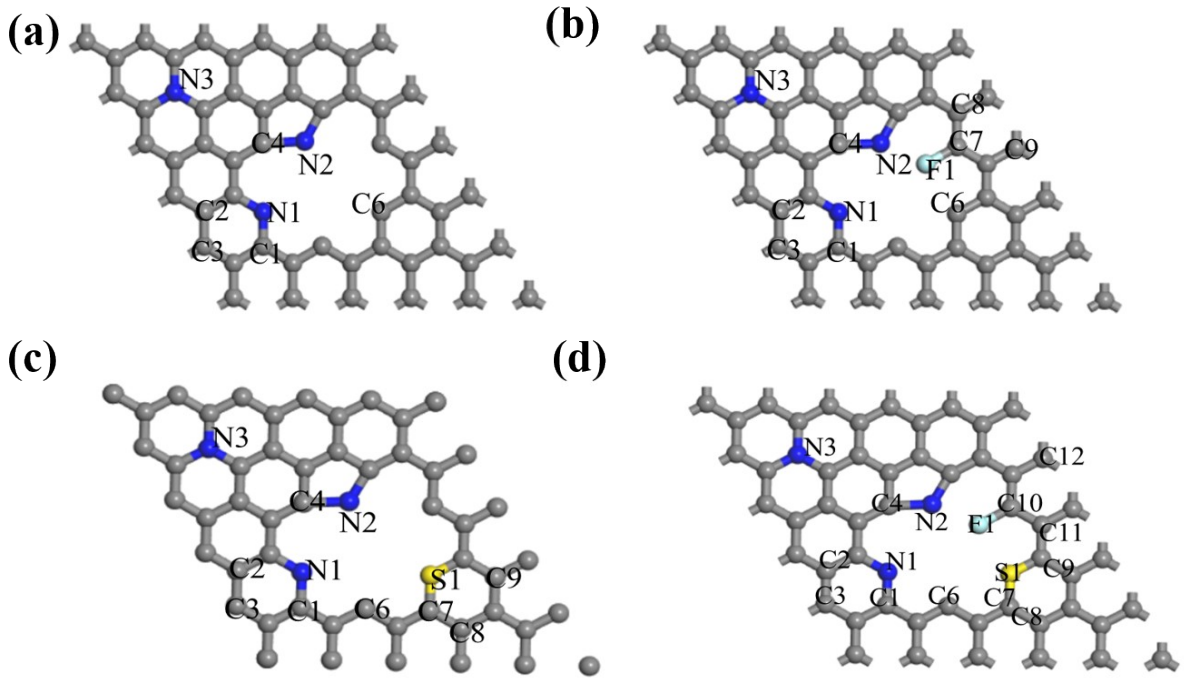

Fig. S10. Possible active sites for adsorption of NaO_2 in (a) N-C, (b) NF-C, (c) NS-C, (d) NFS-C, respectively. In this work, N1 was selected as the adsorption active site of NaO_2 to calculate the free energy for ORR/OER.

6 Supporting Tables

Table S1. Summary of characterization of PAN:PDADMA FSI with different ratio of PAN and PDADMA FSI.

Samples	Weight (g)	Diameter fiber (nm)	Thickness (μm)	Specific Surface area ($m^2\ g^{-1}$)	Fibers volume (cm^3) x10^{-7}	Void space (cm^3) x10^{-7}	I_D/I_G	Discharge capacity ($mAhcm^{-2}$)	Charge capacity ($mAhcm^{-2}$)
PAN:PDADMA FSI 100:0	0.96±0.02	255±5	125±2.9	17.969±0.103	4.4±0.05	43.9±0.14	1.20	0.062±0.015	0.035±0.010
PAN:PDADMA FSI 80:20	1.12±0.03	205±6	114±2.8	21.357±0.099	5.0±0.03	38.9±0.10	1.29	0.078±0.010	0.046±0.021
PAN:PDADMA FSI 70:30	1.20±0.02	140±5	108±2.3	25.627±0.097	5.3±0.01	36.2±0.09	1.32	0.351±0.020	0.099±0.015
PAN:PDADMA FSI 60:40	1.28±0.02	165±5	95±2.7	23.643±0.100	5.7±0.02	30.9±0.12	1.40	0.100±0.018	0.064±0.015

Table S2. Summary of element content of PAN:PDADMA FSI with different ratio of PAN and PDADMA FSI.

Samples	Carbon (C) %	Nitrogen (N) %	Sulphur (S) %	Oxygen (O)%	Fluorine (F) %
PAN:PDADMA FSI 100:0	77.1	1.3	-	21.6	-
PAN:PDADMA FSI 80:20	75.9	1.9	0.51	20.8	0.89
PAN:PDADMA FSI 70:30	74.2	2.3	1.48	20.1	1.92
PAN:PDADMA FSI 60:40	74.6	2	1.33	20.6	1.47

Table S3. Summary of the element content with different configruations within various PAN:PDADMA FSI with different ratio of PAN and PDADMA FSI.

Samples	Percentage within N				Percentage within O		Percentage within S		Percentage within F		
	Pyridinic-N	Pyrrolic-N	Graphitic-N	Oxidized-N	C-O-C	C=O	C-S	S-O	Covalent F-C	Semi-ionic F-C	Ionic F
PAN:PDADMA FSI 100:0	17	32	42	8	20	80	-	-	-	-	-
PAN:PDADMA FSI 80:20	20	23	40	17	26	74	30	70	75	5	20
PAN:PDADMA FSI 70:30	32	22	26	21	48	52	55	45	30	8	62
PAN:PDADMA FSI 60:40	24	20	29	27	39	61	27	73	78	9	13

Table S4 Summary of characterization of varous PAN:PDADMA FSI 70:30 with different thickness.

Thickness (μm)	Weight (g)	Diameter fiber (nm)	Specific Surface area ($m^2\ g^{-1}$)	Fibers volume (cm^3) $x10^{-7}$	Void space (cm^3) $x10^{-7}$	I_D/I_G	Discharge capacity ($mAhcm^{-2}$)	Charge capacity ($mAhcm^{-2}$)
108±2.3	1.20±0.02	140±5	25.627±0.097	5.3±0.01	36.2±0.09	1.32	0.351±0.020	0.099±0.010
230±2.2	2.35±0.03	140±5	22.841±0.098	10.4±0.02	78.1±0.10	1.32	0.364±0.015	0.173±0.015
310±2.1	3.75±0.02	140±5	23.385±0.101	16.7±0.01	102.7±0.08	1.32	0.377±0.021	0.293±0.020

Table S5 Electrochemical Properties of Na-O_2 batteries produced by this work and from recent reported literatures

Air cathode [loading and area]	Electrolyte	% doping	Cycling performance		Reference
			Voltage range (V)	Cyclability, current and limited capacity	
N-doped graphene	0.5M $NaSO_3CF_3$ in diethylene glycol dimethyl ether (DEGDME)	Not mentioned	1.8-3.6	3 cycles, 0.035 mA cm^{-2}, none limited capacity	[8]
N-doped carbon	0.5M $NaSO_3CF_3$ in DEGDME	6.67% Nitrogen	1.5-4.5	100 cycles, 0.5 mAh cm^{-2} at 0.1 mA cm^{-2}	[9]
N-doped carbon	0.5M $NaSO_3CF_3$ in DEGDME	~6% Nitrogen	1.5-4.5	66 cycles, 0.1 mAh cm^{-2} at 0.02 mA cm^{-2}	[10]
N-doped CNF	0.5M $NaSO_3CF_3$ in DEGDME	10.93% Nitrogen	1.5-3.0	90 cycles, 0.04 mAh cm^{-2} at 0.016 mA cm^{-2}	[11]
N-doped carbon	**16.6 mol% NaTFSI in G2/[C_4mpyr][TFSI]**	**2.3% Nitrogen, 1.48% Sulphur, 1.92% Fluorine**	**1.6-3.6**	**157 cycles at 0.1 mA cm^{-2} (85 mA g^{-1}), limited capacity 0.1 and 0.25 mAh cm^{-2}**	**This work**

References

[1] X. Wang, H. Zhu, G.M. Girard, R. Yunis, D.R. MacFarlane, D. Mecerreyes, A.J. Bhattacharyya, P.C. Howlett, M. Forsyth, Preparation and characterization of gel polymer electrolytes using poly (ionic liquids) and high lithium salt concentration ionic liquids, Journal of Materials Chemistry A, 5 (2017) 23844-23852.

[2] H. Li, T.A. Ha, S. Jiang, C. Pozo-Gonzalo, X. Wang, J. Fang, P.C. Howlett, X. Wang, N, F and S doped carbon nanofibers generated from electrospun polymerized ionic liquids for metal-free bifunctional oxygen electrocatalysis, Electrochimica Acta, 377 (2021).

[3] T.A. Ha, A. Fdz De Anastro, N. Ortiz-Vitoriano, J. Fang, D.R. MacFarlane, M. Forsyth, D. Mecerreyes, P.C. Howlett, C. Pozo-Gonzalo, High Coulombic Efficiency Na–O2 Batteries Enabled by a Bilayer Ionogel/Ionic Liquid, The journal of physical chemistry letters, 10 (2019) 7050-7055.

[4] Y. Zhang, N. Ortiz-Vitoriano, B. Acebedo, L. O'Dell, D.R. MacFarlane, T. Rojo, M. Forsyth, P.C. Howlett, C. Pozo-Gonzalo, Elucidating the Impact of Sodium Salt Concentration on the Cathode–Electrolyte Interface of Na–Air Batteries, The Journal of Physical Chemistry C, 122 (2018) 15276-15286.

[5] D.R. Hamann, M. Schlüter, C. Chiang, Norm-Conserving Pseudopotentials, Physical Review Letters, 43 (1979) 1494-1497.

[6] Y.S. Mekonnen, R. Christensen, J.M. Garcia-Lastra, T. Vegge, Thermodynamic and Kinetic Limitations for Peroxide and Superoxide Formation in Na-O2 Batteries, J Phys Chem Lett, 9 (2018) 4413-4419.

[7] Y. Wu, C. Li, W. Liu, H. Li, Y. Gong, L. Niu, X. Liu, C. Sun, S. Xu, Unexpected monoatomic catalytic-host synergetic OER/ORR by graphitic carbon nitride: density functional theory, Nanoscale, 11 (2019) 5064-5071.

[8] Y. Li, H. Yadegari, X. Li, M.N. Banis, R. Li, X. Sun, Superior catalytic activity of nitrogen-doped graphene cathodes for high energy capacity sodium–air batteries, Chemical Communications, 49 (2013) 11731-11733.

[9] S. Zhang, Z. Wen, J. Jin, T. Zhang, J. Yang, C. Chen, Controlling uniform deposition of discharge products at the nanoscale for rechargeable Na–O 2 batteries, Journal of Materials Chemistry A, 4 (2016) 7238-7244.

[10] J.-l. Ma, X.-b. Zhang, Optimized nitrogen-doped carbon with a hierarchically porous structure as a highly efficient cathode for Na–O 2 batteries, Journal of Materials Chemistry A, 4 (2016) 10008-10013.

[11] Z. Zheng, J. Jiang, H. Guo, C. Li, K. Konstantinov, Q. Gu, J. Wang, Tuning NaO2 formation and decomposition routes with nitrogen-doped nanofibers for low overpotential Na-O2 batteries, Nano Energy, 81 (2021) 105529.